Optical Engineering

OpticalEngineering.SPIEDigitalLibrary.org

Two approaches for realizing traceability in nanoscale dimensional metrology

Gaoliang Dai
Ludger Koenders
Jens Fluegge
Harald Bosse

SPIE.

Gaoliang Dai, Ludger Koenders, Jens Fluegge, Harald Bosse, "Two approaches for realizing traceability in nanoscale dimensional metrology," *Opt. Eng.* **55**(9), 091407 (2016), doi: 10.1117/1.OE.55.9.091407.

Downloaded From: http://opticalengineering.spiedigitallibrary.org/ on 04/02/2016 Terms of Use: http://spiedigitallibrary.org/ss/TermsOfUse.aspx

Optical Engineering 55(9), 091407 (September 2016)

Two approaches for realizing traceability in nanoscale dimensional metrology

Gaoliang Dai,* Ludger Koenders, Jens Fluegge, and Harald Bosse
Physikalisch-Technische Bundesanstalt, Bundesallee 100, 38116 Braunschweig, Germany

Abstract. Traceability is a fundamental issue for nanoscale dimensional metrology. The lack of traceability in measurements inhibits the comparison of tools from different manufacturers and limits knowledge about the real size of fabricated features. Two approaches for realizing traceability in nanometrology, referred to as a top-down approach and a bottom-up approach, are presented. Following the top-down approach, for instance, realized using metrological atomic force microscopes, the dimension of nanostructures is derived from the displacement of the scanner, which is directly measured by laser interferometers whose optical frequency is calibrated to an iodine frequency-stabilized laser. Thus, the measurement result is directly traceable with an unbroken chain to the International System of Units—the meter. However, to achieve subnanometer measurement accuracy, which is far smaller than the optical wavelength (632.8 nm in this study), the subdivision of the interference fringe is essential for obtaining desired measurement resolution and accuracy. On the contrary, with the bottom-up approach, the dimension of nanostructures is determined using the silicon crystal lattice as an internal ruler. Due to the small dimension of the crystal lattice constant (e.g., $d_{111} = 0.313$ nm), the bottom-up approach offers measurements with potential highest accuracy. The crystal lattice constant can be traceably calibrated to the meter by, e.g., a combined optical and x-ray interferometer; thus, the traceability of the bottom-up approach is also ensured. The consistency of the two approaches is experimentally confirmed in this paper. *© 2016 Society of Photo-Optical Instrumentation Engineers (SPIE)* [DOI: 10.1117/1.OE.55.9.091407]

Keywords: nanoscale dimensional metrology; traceability; metrological atomic force microscopy; transmission electron microscopy; step height; pitch; critical dimension; metrology.

Paper 160100SS received Jan. 20, 2016; accepted for publication Mar. 2, 2016; published online Mar. 30, 2016.

1 Introduction

Nanoscale dimensional metrology is a key task of developing various nanotechnologies. For instance, in the nanomanufacturing industry, progressive miniaturization of advanced techniques, such as the extreme ultraviolet lithography, nanoimprint, and directed self-assembly, currently delivers nanodevices with feature size below 20 nm. Accurate measurement of the dimensional parameters [including the critical dimension (CD), height, sidewall angle, line-edge roughness/line-width roughness, corner rounding, footing, and so on] of the nanostructures both on silicon wafers and photomasks is a crucial task for process development and process control. As stated in the ITRS metrology roadmap,[1] the measurement uncertainty of the physical CD needs to be reduced to 1.6 nm (year 2016) and 0.7 nm (year 2024).

Traceability is identified as a fundamental challenge of nanometrology.[2] The metrological traceability is defined in the International Vocabulary of Metrology as "property of a measurement result whereby the result can be related to a reference through a documented unbroken chain of calibrations, each contributing to the measurement uncertainty."[3] The lack of traceability in measurements inhibits the comparison of tools from different manufacturers and limits knowledge about the real size of fabricated features.[4]

Taking the semiconductor industry as an example, various measurement tools are being applied for process development and process control, for instance, the optical CD tools,[5,6] critical dimension small-angle x-ray scattering, scanning electron microscopy (SEM),[7] and atomic force microscopy (AFM).[8] The state-of-the-art tools are capable of individual tool reproducibility of far below 1 nm; however, the deviation between the results of different tools on the same set of samples—referred to as the tool-to-tool matching and sample-to-sample measurement bias variation—may exceed several nanometers, remaining as a significant challenge today.[9] This is due to the intrinsic limitations of the individual techniques from either the probe geometry (e.g., in AFMs and SEMs) and/or the modeling errors (e.g., SEMs and scatterometry). To solve this challenge, a feasible approach is to apply traceably calibrated high-quality reference materials, for instance, for calibrating the probe geometry, testing or benchmarking tools, performing comparison measurements between different methods/tools as well as verifying theoretical modeling with experimental results.

Traceability is also crucial for implementation of the hybrid metrology approach[10] in industry. Today different CD tools have their inherent limitations and merits. The concept of the hybrid metrology is to apply different tools in a combined manner, so as to bring together the strengths of different metrology toolsets for providing more comprehensive measurement of the same measurand than any instrument in the ensemble. As the data obtained by these tools must be shared with each other in a complementary or synergistic way for enhancing the metrology capability, the metrology consistency of these tools in the hybrid metrology is an essential issue.

*Address all correspondence to: Gaoliang Dai, E-mail: Gaoliang.dai@ptb.de

0091-3286/2016/$25.00 © 2016 SPIE

Downloaded From: http://opticalengineering.spiedigitallibrary.org/ on 04/02/2016 Terms of Use: http://spiedigitallibrary.org/ss/TermsOfUse.aspx

In this paper, two approaches for realizing traceability in dimensional nanometrology, referred to as a top-down approach (or optical interferometry approach) and a bottom-up approach (or crystal approach), are presented in detail. The consistency of the two approaches is experimentally confirmed.

2 Top-Down Approach

The traceability chain of the top-down approach is illustrated in Fig. 1. The geometric properties of nanostructures being measured can be related to the physical standards that are applied to calibrate the measurement tool. Such physical standards include, for instance, step height, one-dimensional/two-dimensional (1-D/2-D) gratings, or three-dimensional (3-D) pyramid standards, which are available for calibrating the scaling factors of the vertical and lateral axes of the measurement tools.[11] Prior to their usage, these physical standards are usually calibrated by metrology tools such as diffractometer (for lateral standards),[12] interference microscopy (for height standards),[13] or metrological AFM with built-in interferometers (for lateral, height, and 3-D standards).[14] According to the wave optic theory, the measurement results of these metrology tools can be directly related to the wavelength (λ) of the applied optical source, which can in turn be linked to the SI unit meter, as the optical frequency is calibrated either to an iodine frequency stabilized laser or an optical frequency comb.[15] Through such an unbroken calibration chain described above, the traceability of dimensional properties of nanostructures can be ensured.

Today more and more metrological AFMs[14,16–18] have been built up and are becoming a kind of major nanometrology tool. They have outstanding metrology properties, such as high lateral and vertical resolution, low measurement uncertainty, and nondestructive and 3-D measurement capability, offering high calibration versatility for nanometrology.

To demonstrate such a metrological AFM, we introduced in this paper a metrological large-range AFM (Met.LR-AFM) developed at Physikalisch-Technische Bundesanstalt (PTB), which has a capable measurement volume of 25 mm × 25 mm × 5 mm.[14] The schematic diagram and the photo of the instrument are shown in Figs. 2(a) and 2(b), respectively. In the instrument, the sample (S) is fixed on a piezo stage (PZT stage), which is in turn mounted on a mirror corner, which is a motion platform of a high-precision mechanical stage referred to as a nanopositioning and nanomeasuring machine (NMM).[19] The mirror corner is moved by stacked mechanical x-, y-, and z-stages, which offer a motion range of 25, 25, and 5 mm, respectively.

The Met.LR-AFM measures in the so-called scanning sample principle. During measurements, the sample is scanned in the xy-plane at the given speed and is servo controlled along the z-axis to keep the AFM tip–sample interaction to be constant. In such a way, the geometry of the nanostructure can be derived from the x-, y-, and z-coordinates of the scanner, in a principle similar to coordinate measuring machines. The Met.LR-AFM may work in the contact, noncontact, or intermittent contact mode. The static deformation or dynamic properties of the cantilever, which is related to the tip–sample interaction, is detected using an optical lever.

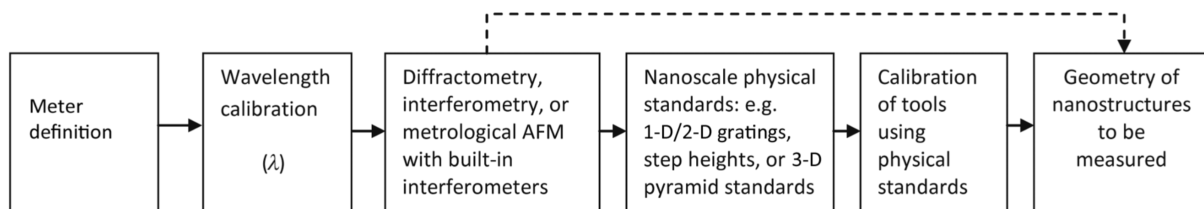

Fig. 1 Traceability chain of nanoscale dimensional metrology with top-down approach.

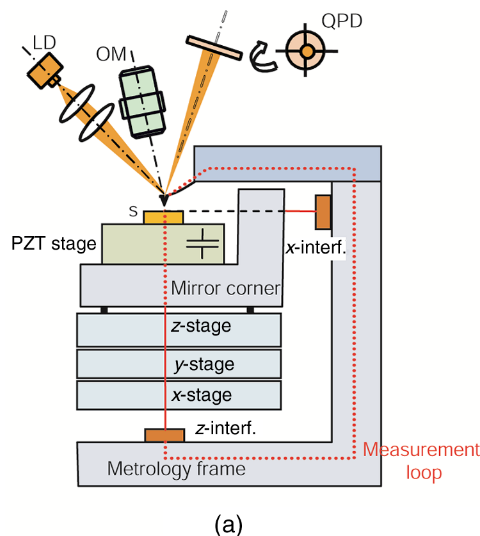

(a)

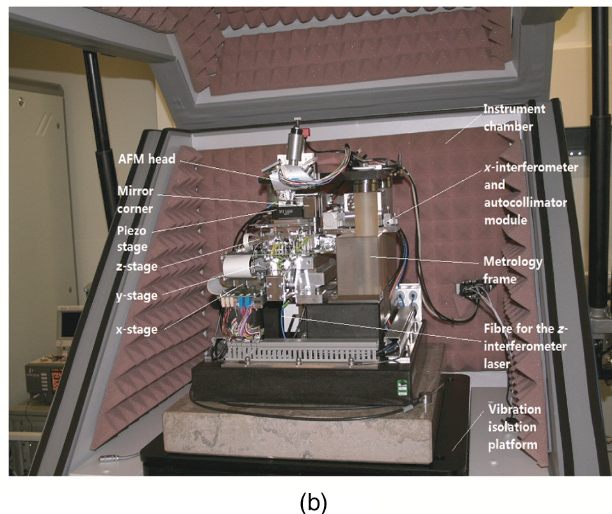

(b)

Fig. 2 Met.LR-AFM developed at PTB applicable for traceable nanoscale dimensional calibrations, shown as (a) schematic diagram and (b) photo of the instrument.

Downloaded From: http://opticalengineering.spiedigitallibrary.org/ on 04/02/2016 Terms of Use: http://spiedigitallibrary.org/ss/TermsOfUse.aspx

Instead of nanometric positioning sensors, such as capacitive sensor, strain gauge, or linear variable differential transducer (LVDT) applied in commercial AFMs, metrological AFMs typically apply laser interferometers for measuring the scanner motion for direct traceability. In the Met.LR-AFM, three interferometers [only that of x- and z-axes are shown in Fig. 2(a)] and two autocollimators (not shown in figure) measure the six degrees of freedom of the mirror corner stage with respect to the metrology frame. By servo controlling the position and angles of the mirror corner stage, the NMM can either measure or position the sample with nanometer accuracy.[19] The measurement loop of the instrument is shown as the red dot lines.

The principle of the nanometric displacement measuring interferometer built-in in the NMM is shown in Fig. 3. It is a Michelson type interferometer with plane reference mirror (RM) and measurement mirror (MM). The incident laser beam is polarized by a polarizer located in the 45-deg orientation and is then split into two beams with s- and p-polarizations by a polarizing beam splitter (PBS) forming the reference and measurement beams, respectively. The reflected reference beam (s-polarization) is turned into a circular polarization beam by a quarter wave plate (QWP) whose fast axis is oriented at 45 deg. After being reflected by the RM and passing the QWP the second time, the reference beam is turned into a p-polarization and thus passes through the PBS. Similarly, after the measurement beam (p-polarization) passed through a QWP, being reflected at MM and then passed the QWP the second time, it is changed into s-polarization and is reflected at the PBS, and thus recombined with the reference beam forming the interference. The recombined beam is divided by a beam splitter (BS) into two detection beams, which after passing a pair of polarizers rotated 45 deg relative to each other are detected by the photo detectors PD1 and PD2, and a pair of 90 deg phase-shifted signal $S_{\cos}$ and $S_{\sin}$ is obtained. Such a signal pair forms a circular Lissajous figure where the phase shift (Φ) of the interferometer can be determined. The displacement of the MM can be calculated as

$$L = \frac{\lambda}{2n}\left(m + \frac{\varnothing}{4\pi}\right), \tag{1}$$

where λ is the vacuum wavelength of the applied laser source, n is the air refractive index, m is the measured integer number of interference fringes, and Φ is the measured phase indicating the fractional interference fringe.

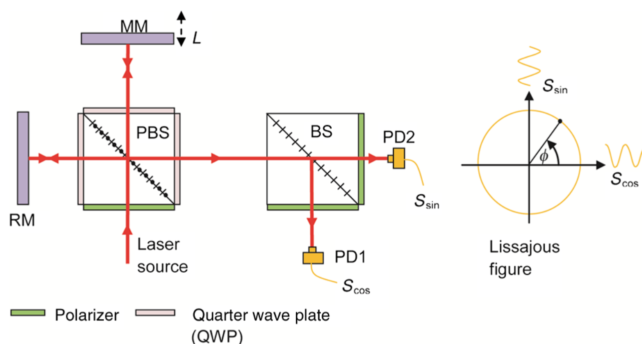

Fig. 3 Measuring principle of the nanometric displacement interferometer built in the NMM.

In the Met.LR-AFM, the air refractive index (n) is determined by applying the Ciddor equation [20] with measured environmental parameters (air temperature, air pressure, and humidity). As the measurement setup is located in a good instrument chamber, the air temperature gradient and air turbulence is kept small; thus, the change of air refractive index is slow and can be determined with quite high accuracy (better than 1×10^{-7}). The wavelength of our working lasers (frequency stabilized He–Ne lasers) is calibrated by the iodine frequency stabilized laser at PTB as $(632\,991\,234 \pm 5)$ fm. The optical frequency variation over a time period of 80 h is measured to be below 6 MHz, i.e., $<1.3 \times 10^{-8}$.

With the calibrated λ and n, the displacement of the measurement mirror (i.e., the stage motion) can be measured accurately and with direct traceability to the SI unit meter. Consequently, the measured dimensional parameters of nanostructures are also traceable, since the scales of the measured data are ultimately derived from the displacement of the stage.

We named this traceability approach as a top-down approach due to two facts. First, compared to the size and the measurement volume of the instrument, the size of the nanostructure is much smaller. Second, in the metrology tool, it is the laser wavelength that actually acts as the measurement ruler. As the wavelength is much larger than the desired measurement resolution/accuracy typically at sub-nanometer level in nanometrology, the subdivision of the scale by interpolation of interference fringes is needed. It leads to another challenging issue, namely the inherent nonlinearity error of optical interferometers.

Today metrology AFMs are widely applied for accurate and traceable calibrations of, for instance, step height and depth setting standards, lateral standards (1-D/2-D gratings), nano flatness standards, 3-D pyramid standards, roughness standards as well as 3-D form of nanostructures.[21] As an example, Fig. 4 presents the pitch calibration of a 2-D1000 grating with a nominal pitch value of 1000 nm. The 3-D view of the measured AFM image is shown in Fig. 4(a), and the evaluated deviations of the center of gravity of the grid structures from their ideal position is plotted in Fig. 4(b). Results from five repeated measurements taken at the same region of the grating are plotted, indicating good measurement reproducibility. It should be mentioned that the results mainly reflect the imperfections in the sample itself, as the metrology performance of the Met.LR-AFM is actually much better than that. Typically, it has a relative measurement accuracy up to 1 to 2×10^{-5} for the mean pitch value of gratings.

3 Bottom-Up Approach

With the development of modern spherical aberration correction technique, currently the (scanning) transmission electron microscopes [(S)TEMs] are capable of microscopic imaging and microanalysis with a spatial resolution down to 0.05 nm, i.e., true atomic resolution. Such outstanding imaging power offers new solutions for nanometrology. As illustrated in Fig. 5, if the atoms in the nanostructures are resolvable, its dimensional parameters (shown as the line width) can be easily determined by using the atom spacing as an internal ruler. A remarkable progress applying this idea is the development of single crystal CD reference material by

Downloaded From: http://opticalengineering.spiedigitallibrary.org/ on 04/02/2016 Terms of Use: http://spiedigitallibrary.org/ss/TermsOfUse.aspx

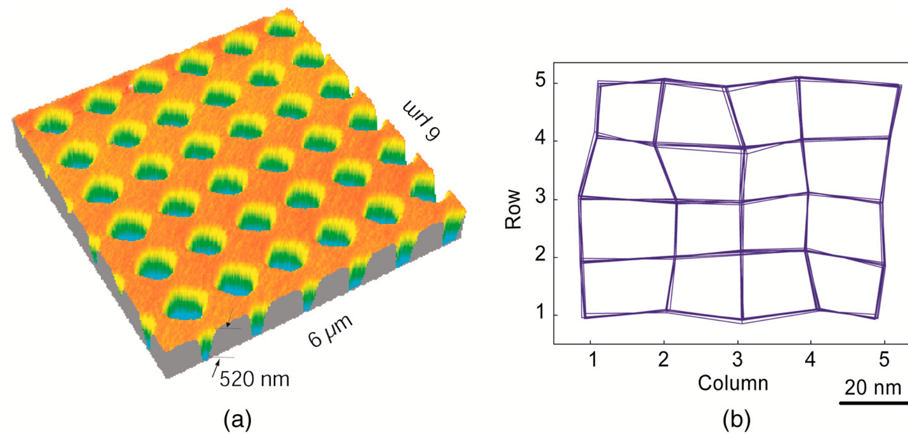

Fig. 4 Calibration of the pitch of a 2-D 1000 grating by the Met.LR-AFM, shown as (a) a 3-D view of the measured AFM image and (b) the evaluated deviation of the gravity center of the measured 2-D grating grid from its ideal position. Results from five repeated measurements are plotted, indicating the good measurement reproducibility.

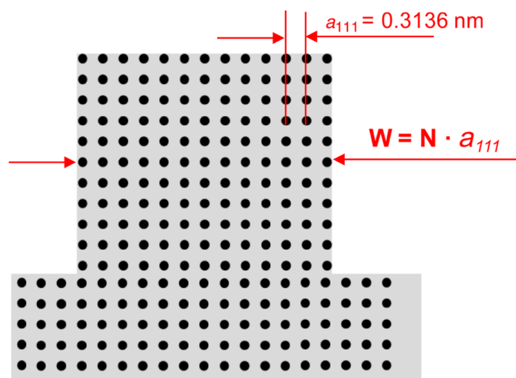

Fig. 5 Basic idea for the determination of feature width using the crystal lattice constant as an internal ruler.

Dixson et al.[22] Later, Takamasu et al.[23] and our group[24] have also utilized this idea for traceable and high accurate line width metrology.

A measurement example is presented in Fig. 6 to demonstrate the measurement power of the idea presented above. Before the measurement, a line feature made of a single crystal silicon sample is prepared using a dual-beam focused ion beam (FIB) instrument (Helios nanolab 660 of FEI) at the target measurement location. To protect the target feature not being influenced during the sample preparation, two protection layers (first a carbon layer followed by a platinum layer) are deposited to the target feature before the TEM lamella is prepared. Lamellas were produced utilizing the FIB lift out technique. The lamellas were further thinned to have a thickness of ~50 nm using 2 kV Ga+ ions before being measured in TEM.

Figure 6(a) shows the STEM image of the line feature measured in a high-end TEM device (Titan Themis 300 of FEI) at a magnification of 910k and with a resolution of 22.5 pm/pixel. The structure at the top-left corner in the marked box is zoomed in and shown in Fig. 6(b). The crystal planes of {1 1 1} can be well resolved. As shown in the figure, the atom spacing between the crystal planes {1 1 1}, a_{111}, which was calculated traceably as 313.560 11(17) pm from the d_{220} value determined by combined x-ray and optical interferometry,[25] can be used as an internal ruler for measurements.

To apply the bottom-up approach in practice, it remains as a challenging issue to accurately assign the feature edges in high-resolution (S)TEM images. Different methods have been developed.[22–24,26,27] One method is to define the edge as the end of Si lattice structure between the Si lattice and silicon oxide film.[22,23] It, however, encounters two problems in practice. First, the contrast of fringes will appear dimmed near the boundary, leading to questionable edge location areas.[22] To mitigate this issue, an averaging method by applying Si lattice pattern has been applied in Ref. 23. But it demands that the obtained TEM image offers true atomic resolution, which unfortunately cannot always be satisfied. Second, only the boundary between the Si-SiOx (the curve $B_{Si\text{-}SiOx}$ shown in the figure) is determined using the method; however, the boundary between the SiOx-C (the curve $B_{SiOx\text{-}C}$ shown in the figure) is usually the real physical boundary, e.g., when the feature is measured by AFMs. To determine the needed boundary of SiOx-C, it is usually expanded by an estimated thickness value of the silicon oxide layer. Consequently, the uncertainty of the thickness value directly impacts the measurement result. Alternatively, the half intensity[26] or the maximum intensity gradient[27] method is also applied for defining the edge. As different definitions will lead to different results, consequently it raised a fundamental question: which definition agrees better with the physical edge of the structure?

We had investigated this issue in our previous study.[24] Our conclusion suggested that the feature edge should be better defined as the half intensity position for STEM images. The definition is analogous to the edge assignment issue in conventional optical microscopic images measured with an incoherent light source. Physically, it stands for the edge location where the material occupation is about 1:1. This edge definition is adopted in this study, and the width of the line feature is determined as (44.3 ± 0.3) nm for the example shown in Fig. 6. This result is also traceable to the SI unit of meter via an unbroken calibration chain. It is worth mentioning that the uncertainty is driven much more by determining the edge position of the SiOx-C boundary than the lattice spacing.

Downloaded From: http://opticalengineering.spiedigitallibrary.org/ on 04/02/2016 Terms of Use: http://spiedigitallibrary.org/ss/TermsOfUse.aspx

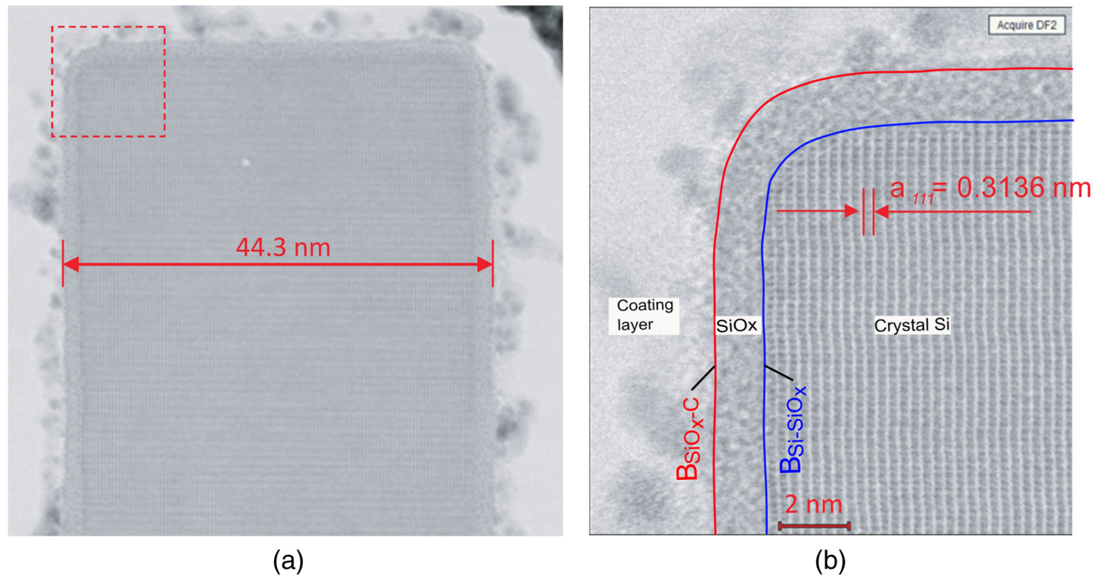

Fig. 6 Width of a crystal silicon line feature determined by the bottom-up approach, shown as (a) the measured STEM image of the line feature and (b) the zoom-in view of the image at the marked box in (a), where the crystal plane is clearly visible for being applied as an internal ruler.

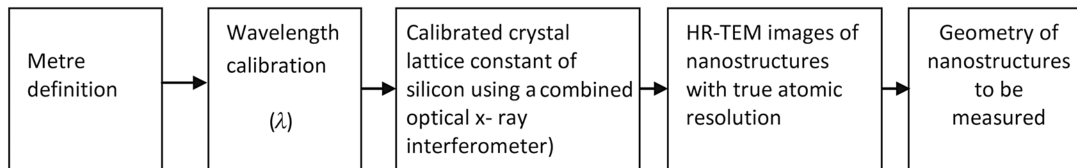

Fig. 7 Traceability chain of nanoscale dimensional metrology with bottom-up approach.

Based on the research works achieved above, recently CIPM CCL (International Committee for Weights and Measures, Consultative Committee for Length) working group on dimensional nanometrology (CCL WG-N) has proposed to use TEM and the reference value of the bulk silicon lattice constant as a pathway for traceability to the SI meter for applications in dimensional nanometrology.[28] We name this crystal approach as a bottom-up approach, since compared to the top-down approach where the optical wavelength is used as the physical ruler, in this approach, the physical ruler—the atom spacing—is much smaller. It also fits nature regarding how the structure is formed.

We summarize the traceability chain of the bottom-up approach in Fig. 7. Nanostructures are first measured with high-resolution TEM with true atomic resolution; thus, their geometry can be related to the lattice constant of the crystal, which is calibrated to standard optical wavelength using, e.g., a combined optical and x-ray interferometer. Similar to the top-down approach, the optical wavelength is calibrated to the SI unit meter via either an optical frequency comb or an iodine frequency stabilized laser.

4 Comparison of Two Approaches

Comparing the two different traceability approaches, a fundamental question is if they are consistent with each other or not. To verify this issue, we have designed a measurement experiment where a same line width structure is measured using two different approaches. The line width structure is made of single crystal silicon as shown in Fig. 8. The measurement of its line width using the bottom-up approach is the same as shown in Figs. 5 and 6. To determine the line width using the top-down traceability approach, we calibrated the pitch p of line features using our Met.LR-AFM before the feature being sample prepared for TEM measurements. After the line features were STEM imaged as shown in Fig. 8, we again derived the line width related to the calibrated pitch as $W1 * p/D$ and $W2 * p/D$, where $W1$ and $W2$ are the widths and D is the pitch of line features evaluated from the STEM image in the unit of pixels, respectively. The measured line widths using two different approaches are compared in Table 1; the agreement is better than 0.3 nm, confirming the consistency of the two approaches.

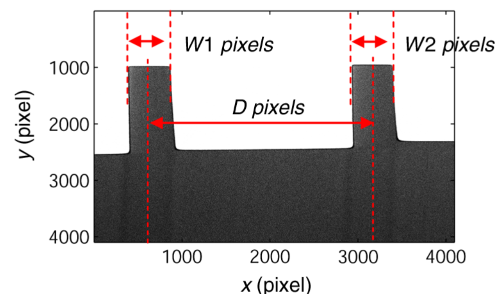

Fig. 8 Calibration of the feature width with traceability via the pitch of a line pair, which was calibrated by a metrological AFM using the top-down approach.

Downloaded From: http://opticalengineering.spiedigitallibrary.org/ on 04/02/2016 Terms of Use: http://spiedigitallibrary.org/ss/TermsOfUse.aspx

Table 1 Comparison of line width measurement results using two different traceability approaches: the top-down and bottom-up. All data are in nm.

Line feature no.	1	2	3	4	5
Crystal lattice constant method (bottom-up approach)	99.33	93.94	100.71	96.34	93.16
Pitch method (top-down approach)	99.59	93.92	100.71	96.14	93
Difference	−0.26	0.02	0	0.20	0.16

It should be stressed that using metrological tools such as AFM and SEM for nanometrology, the traceability of their scanner's displacement is ensured by optical interferometry. For some measurands (e.g., line width, corner radius, and so on), the measurement results are related not only to the properties of the scanners, but also to the tip–sample interaction. For ensuring the traceability for such measurements, the tip related issues also need to be calibrated traceably.

A measurement example is shown in Fig. 9. In this measurement, a group of five line features with nominal feature width of 50, 70, 90, 110, and 130 nm, respectively, is first measured using a CD-AFM[8] using the top-down approach and then a TEM device using the bottom-up approach. The CD-AFM was traceably calibrated using a set of step height and lateral standards to the Met.LR-AFM. Figure 9(a) plots the apparent CD-AFM results (without tip correction) shown as the y data with respect to the TEM results shown as the x data. By linear regression of the measured data, we get $y = 0.9988\,x + 128.32$ nm with x in nm. The result confirms the consistency of the measurement scale of both approaches; however, it also reveals an offset of 128.32 nm, which is attributed to the tip geometry and the tip–sample interaction in the CD-AFM measurements. Physically, it has been well understood since in AFM measurement, the profile obtained is the dilated result of the real structure by the (effective) tip geometry,[29] as shown in Fig. 9(b). Consequently, to ensure traceable line width measurement results in CD-AFMs, not only the scale factors but also its (effective) tip geometry needs to be calibrated traceably. We had reported the development of a kind of line width standard that is suitable for such purpose,[30] where the traceability of its calibration is based on the bottom-up approach. With the characterized (effective) tip geometry, the tip-induced dilation in the apparent results can be compensated. In the given measurement example, the (effective) tip width can be regarded as a zeroth-order component[4] and the compensation can be performed by subtracting the offset value of 128.32 nm from the apparent CD measurement results.

5 Conclusion

Traceability is a fundamental issue for nanoscale dimensional metrology. In the nanomanufacturing industry, for instance, the traceability is needed to make the results of different measurement tools comparable, to allow data fusion, and to understand the real size of the fabricated nanostructures.

Two traceability approaches have been presented in the paper: the top-down approach (or optical interferometry approach) and the bottom-up approach (or crystal approach). The top-down approach is based on optical interferometry, which is usually built-in in metrological tools, for instance, metrological AFMs. AFM images of nanostructure measured in such tools are derived from the displacement of their scanner, which is precisely measured by nanometric laser interferometers. Thus, the measurement results can be related to the wavelength of the laser source calibrated to the SI unit meter using either an optical frequency comb or an iodine frequency stabilized laser. In the bottom-up approach, the measurement is performed using the atom spacing as a physical ruler. The atom spacing can be calibrated to the SI unit meter using, e.g., a combined optical and x-ray interferometer.

The two traceability approaches we have described both have advantages and disadvantages. The bottom-up approach uses the atom spacing as a ruler, which is much shorter than the optical wavelength; therefore, it is capable of much higher measurement resolution and accuracy. In

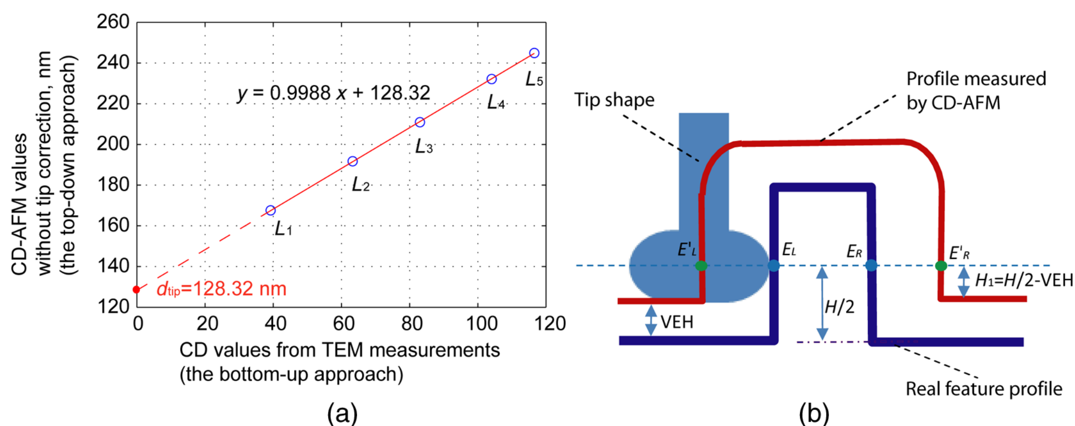

Fig. 9 (a) Comparison of the feature width of five line features measured by a CD-AFM (the top-down approach) without tip correction and the results obtained by TEM measurements (the bottom-up approach) and (b) schematic diagram showing the dilation of the measured nanostructure by the tip geometry only. E_L and E_R indicate the tip–sample interaction points at the middle height ($H/2$) of the feature, while the center positions of the tip, E'_L and E'_R, are registered as the measurement result. VEH indicates the so-called vertical edge height of the tip.

Downloaded From: http://opticalengineering.spiedigitallibrary.org/ on 04/02/2016 Terms of Use: http://spiedigitallibrary.org/ss/TermsOfUse.aspx

addition, thanks to the true atomic resolution power, the measurement results suffer much less from probe–sample interaction than that of other measurement tools (for instance, AFM, SEM, and optical scatterometry). However, using the bottom-up approach, the sample material needs to be a perfect single crystal structure. The measurable feature size is limited since it is difficult to obtain true atomic resolution over a large imaging range. In addition, the low throughput of the TEM measurements and the destructive nature of the sample preparation also limited its practical applications. In contrast, the top-down approach is easier to be used, applicable for large feature size, and (almost) nondestructive. However, as the optical wavelength is typically at the order of several 100 nm, precise interpolation of interference fringes is necessary and the nonlinearity error of the interferometer becomes a challenge. Furthermore, the measurement bias due to tip–sample interaction could be a critical issue for some measurements.

Two traceability approaches introduced in this paper can not only be applied separately, but also be used in a joint manner for more calibration capabilities, especially in understanding the complicated tip–sample interaction issues.

References

1. Table MET3, "Lithography Metrology (Wafer) Technology Requirements," https://www.dropbox.com/sh/49tu7ip2lsf4922/AABbCC9_QEnzE7U2pocEUza7a/2012Tables/Metrology_2012Tables.xlsx?dl=0 (19 March 2016).
2. EURAMET e.V., "Strategic research agenda for metrology in Europe," Version 1.0 (2015).
3. BIPM, "International vocabulary of metrology—basic and general concepts and associated terms (VIM)," 2012, www.bipm.org/utils/common/documents/jcgm/JCGM_200_2012.pdf (4 March 2016).
4. N. G. Orji and R. G. Dixson, "Higher order tip effects in traceable CD-AFM based linewidth measurements," *Meas. Sci. Technol.* **18**, 448–455 (2007).
5. C. J. Raymond et al., "Metrology of subwavelength photoresist gratings using optical scatterometry," *J. Vac. Sci. Technol. B* **13**(4), 1484–1495 (1995).
6. Z. Yu, H. Gao, and S. Y. Chou, "*In situ* real time process characterization in nanoimprint lithography using time-resolved diffractive scatterometry," *Appl. Phys. Lett.* **85**, 4166 (2004).
7. W. Häßler-Grohne and H. Bosse, "Electron optical metrology system for pattern placement measurements," *Meas. Sci. Technol.* **9**, 1120–1128 (1998).
8. G. Dai et al., "New developments at Physikalisch Technische Bundesanstalt in three-dimensional atomic force microscopy with tapping and torsion atomic force microscopy mode and vector approach probing strategy," *J. Micro/Nanolith. MEMS MOEMS* **11**(1), 011004 (2012).
9. V. Ukraintsev and B. Banke, "Review of reference metrology for nanotechnology: significance, challenges, and solutions," *J. Micro/Nanolith. MEMS MOEMS* **11**(1), 011010 (2012).
10. R. Silver et al., "Improving optical measurement accuracy using multi-technique nested uncertainties," *Proc. SPIE* **7272**, 727202 (2009).
11. G. Wilkening and L. Koenders, Eds., *Nanoscale Calibration Standards and Methods: Dimensional and Related Measurements in the Micro and Nanometer Range*, Wiley-VCH, Weinhheim (2005).
12. E. Buhr et al., "Multi-wavelength VIS/UV optical diffractometer for high-accuracy calibration of nano-scale pitch standards," *Meas. Sci. Technol.* **18**, 667–674 (2007).
13. H. Haitjema, "International comparison of depth-setting standards," *Metrologia* **34**, 161 (1997).
14. G. Dai et al., "A metrological large range atomic force microscope with improved performance," *Rev. Sci. Instrum.* **80**, 043702 (2009).
15. E. Benkler, F. Rohde, and H. R. Telle, "Robust interferometric frequency lock between cw lasers and optical frequency combs," *Opt. Lett.* **38**, 555–557 (2013).
16. F. Meli and R. Thalmann, "Long-range AFM profiler used for accurate pitch measurements," *Meas. Sci. Technol.* **9**, 1087–1092 (1998).
17. S. Gonda et al., "Real-time, interferometrically measuring atomic force microscope for direct calibration of standards," *Rev. Sci. Instrum.* **70**, 3362–3368 (1999).
18. J. Haycocks and K. Jackson, "Traceable calibration of transfer standards for scanning probe microscopy," *Precis. Eng.* **29**, 168–175 (2005).
19. E. Manske et al., "New applications of the nanopositioning and nanomeasuring machine by using advanced tactile and non-tactile probes," *Meas. Sci. Technol.* **18**, 520 (2007).
20. P. E. Ciddor, "Refractive index of air: new equations for the visible and near infrared," *Appl. Opt.* **35**, 1566–1573 (1996).
21. G. Dai, F. Pohlenz, and M. Xu, "Accurate and traceable measurement of nano- and microstructures," *Meas. Sci. Technol.* **17**, 545 (2006).
22. R. G. Dixson et al., "Traceable calibration of critical-dimension atomic force microscope linewidth measurements with nanometer uncertainty," *J. Vac. Sci. Technol. B* **23**(6), 3028–3032 (2005).
23. K. Takamasu et al., "Sub-nanometer calibration of CD-SEM line width by using STEM," *Proc. SPIE* **7638**, 76381K (2010).
24. G. Dai et al., "Reference nano-dimensional metrology by scanning transmission electron microscopy," *Meas. Sci. Technol.* **24**, 085001 (2013).
25. E. Massa et al., "Measurement of the lattice parameter of a silicon crystal," *New J. Phys.* **11**, 053013 (2009).
26. K. Takamasu et al., "Edge determination methodology for cross-section STEM image of photoresist feature used for reference metrology," *Proc. SPIE* **8681**, 868132 (2013).
27. K. Takamasu et al., "Sidewall roughness and line profile measurement of photoresist and FinFET features by cross-section STEM and TEM image for reference metrology," *Proc. SPIE* **9050**, 90501K (2014).
28. R. Dixson and H. Bosse, "Recommendations of CCL/WG-N: realization of SI meter using silicon lattice and transmission electron microscopy for dimensional nanometrology," (to be published).
29. J. S. Villarrubia, "Algorithms for scanned probe microscope image simulation, surface reconstruction, and tip estimation," *J. Res. Nat. Inst. Stand. Technol.* **102**, 425 (1997).
30. G. Dai et al., "Development and characterisation of a new line width reference material," *Meas. Sci. Technol.* **26**, 115006 (2015).

Biographies for the authors are not available.

Downloaded From: http://opticalengineering.spiedigitallibrary.org/ on 04/02/2016 Terms of Use: http://spiedigitallibrary.org/ss/TermsOfUse.aspx